Electronic Supplementary Material (ESI) for Physical Chemistry Chemical Physics.

Supporting Information

Using coarse-grained molecular dynamics to understand the effect of ionic liquids on the aggregation of Pluronic copolymer solutions

Germán Pérez-Sánchez[a,*], Nicolas Schaeffer[a], André M. Lopes[b],

Jorge F. B. Pereira[c] and João A. P. Coutinho[a]

[a]CICECO – Aveiro Institute of Materials, Department of Chemistry, University of Aveiro, 3810-1933 - Aveiro, Portugal

[b]Faculty of Pharmaceutical Sciences, University of Campinas, Campinas, SP, Brazil.

[c]Univ Coimbra, CIEPQPF, Department of Chemical Engineering, Rua Sílvio Lima, Pólo II – Pinhal de Marrocos, 3030-790 Coimbra, Portugal

[*]Corresponding author:

Prof. Germán Pérez-Sánchez

gperez@ua.pt (Phone: +351-234-370200)

Aveiro Institute of Materials, Department of Chemistry,

University of Aveiro

Table of contents

Note about the selected coarse-grained MARTINI parameters for the choline and hexanoate anions:

For the hexanoate cation, the C_1 CG bead from MARTINI was selected for the alkyl fragment since was developed to mimic a butyl chain[1] which was also widely used to model the alkyl-chain of many surfactant moieties. For the hexanoate carbonyl charged group we have only four options for charged moieties in the MARTINI model, Q_a, Q_d, Q_{da} and Q_0 depending on the hydrogen bonding capabilities namely, acceptor, donor, donor&acceptor and none, respectively. Thus, for the carbonyl group the option was Q_a with the hydrogen bond acceptor capability.

Finally, for the choline molecule, the MARTINI CG Q_0 charged with non-hydrogen bonding capability was selected for the nitrogen charged center surrounded by three methyl groups since this configuration was successfully validated and used. The Q_0 CG bead was previously used to symbolise the charged headgroup of the cetyltrimethylammonium bromide (C_{16}TAB) in previous studies[2–7] among others. For the polar choline region, the polar CG bead type "P" available in MARTINI was the only option. It must be noticing that five degrees for the polarity strength can be selected, from 1 to 5 exhibiting the level 1 the lowest polarity. In this regard, the available polar degrees were attempted being the P_1 the one that better assessed the AA behaviour when the RDFs were analysed. The RDFs AA-CG comparison was used to evaluate the ability of the selected CG beads to reproduce the AA behaviour as shown in **Figures S1 and S2**.

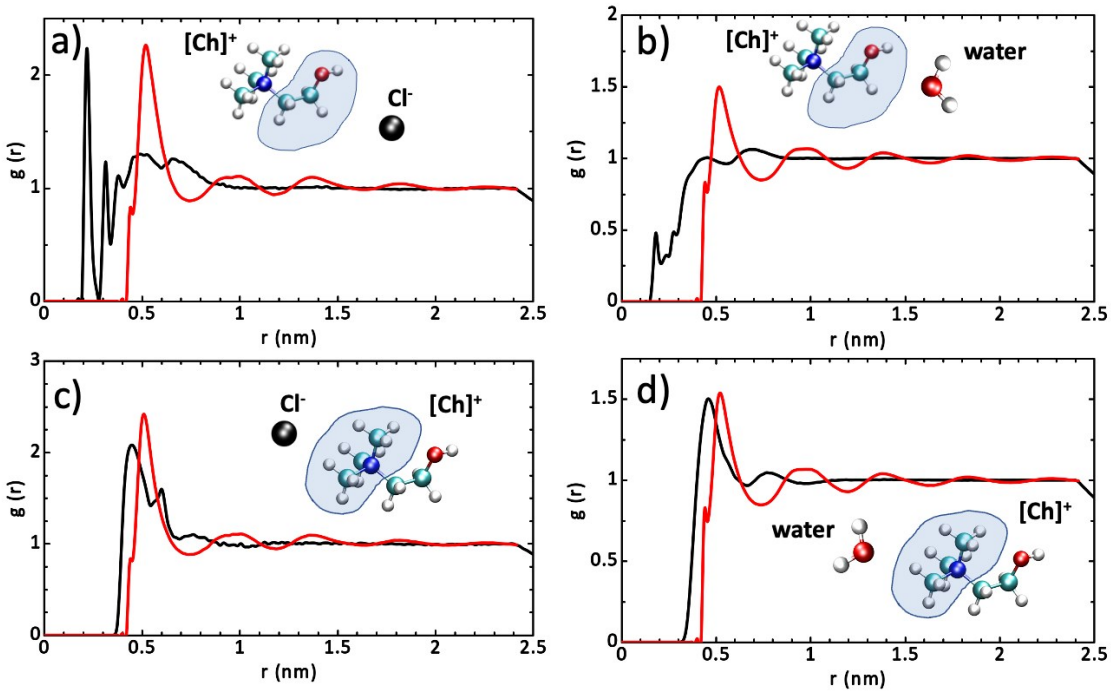

Figure S1. Radial distributions functions (RDFs) for the [Ch]Cl aqueous solutions obtained in the run1 AA (black) and run2 CG (red) systems. The insets show the $[Ch]^+$ regions selected in the calculation. The RDFs for the CG systems were normalised taking into account the 4:1 atom mapping. a) RDFs between hydroxyl $[Ch]^+$ group and the Cl^-, b) RDFs between hydroxyl $[Ch]^+$ group and the H_2O, c) RDFs between amine $[Ch]^+$ group and the Cl^-, d) RDFs between amine $[Ch]^+$ group and H_2O.

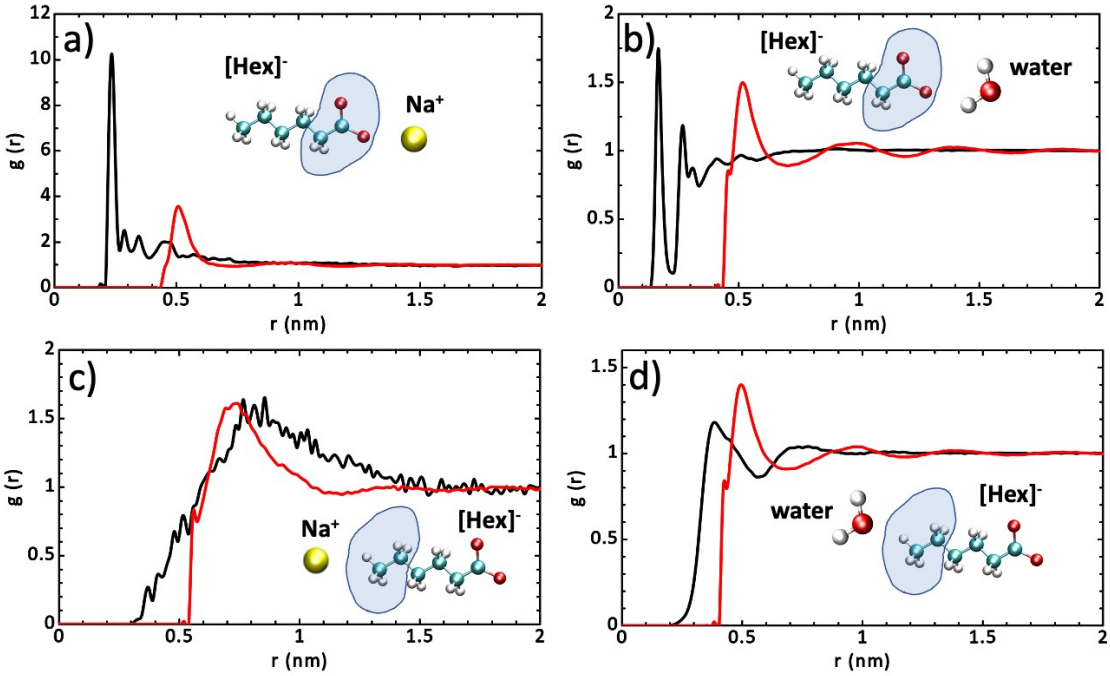

Figure S2. Radial distributions functions (RDFs) for the Na[Hex] aqueous solutions obtained in the run3 AA (black) and run4 CG (red) systems. The insets show the $[Hex]^-$ regions selected in the calculation. The RDFs for the CG systems were normalised taking into account the 4:1 atom mapping. a) RDFs between the $[Hex]^-$ carboxyl group and the Na^+, b) RDFs between $[Hex]^-$ carboxyl group and the H_2O, c) RDFs between terminal alkyl-chain $[Hex]^-$ groups and the Na^+, d) RDFs between terminal alkyl-chain $[Hex]^-$ groups and H_2O.

Table S1. Densities of the atomistic and coarse-grained [Ch]Cl and Na[Hex] aqueous solution found in the MD simulations to validate the coarse-grained model. The ρ^{sim} and ρ^{exp} are the densities obtained in the simulations and literature experimental references, respectively.

Simulation	Systems	ρ^{sim}	ρ^{exp}
run1[a]	[Ch]Cl AA	1.035 ± 0.004	1.020[c]
run2[a]	[Ch]Cl CG	1.088 ± 0.01	-
run3[b]	Na[Hex] AA	1.020 ± 0.008	0.923[d]
run4[b]	Na[Hex] CG	0.96 ± 0.01	-

[a]20 %wt of [Ch]Cl, [b]M=0.5 of Na[Hex]$^-$ [c]Maginn *et al.*[8], [d]Fotouhabadi *et al.*[9]

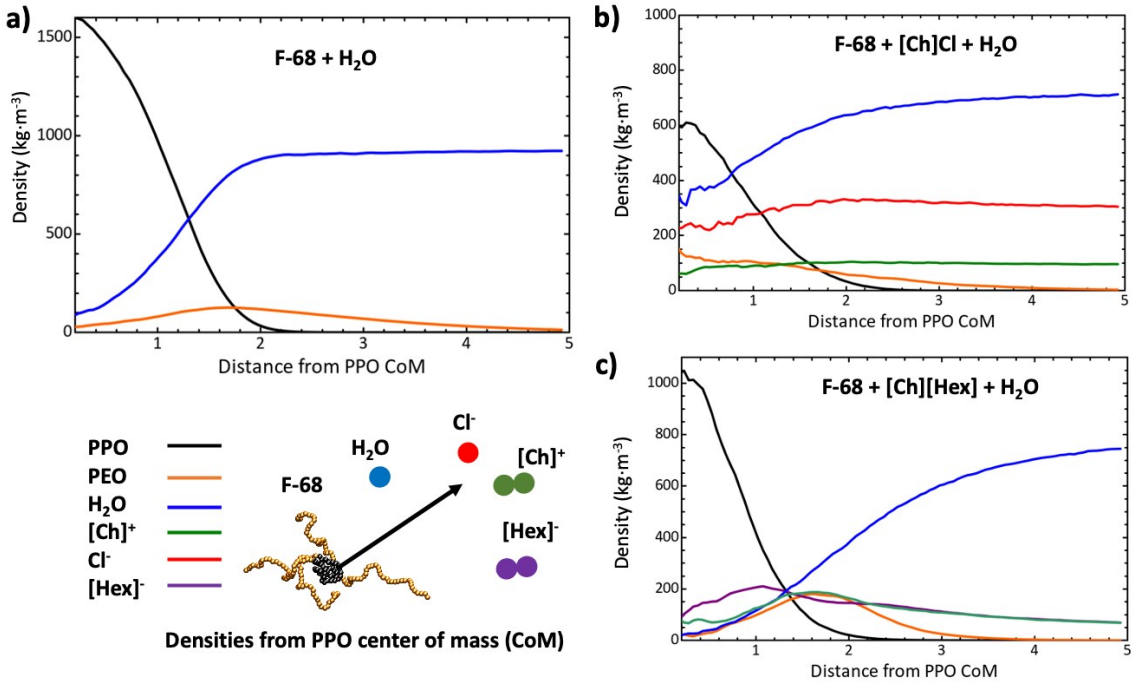

Figure S3. Density profiles for the F-68 aggregates taking the poly(propylene oxide) block (PPO) as the center of mass for the F-68 aqueous solution (run5) and the mixtures with [Ch]Cl (run6) and [Ch][Hex] (run7).

Table S2. Details of the MD simulations carried out for the F-68 and the L-35 aqueous solution and their mixtures with [Ch]Cl and [Ch][Hex]. The F-68 concentration is 1 wt%, 2.75 mol dm^{-3} and 0.6 mol dm^{-3} for [Ch]Cl and [Ch][Hex], respectively. The L-35 concentration is 1 wt%, 1 mol dm^{-3} and 0.15 mol dm^{-3} for [Ch]Cl and [Ch][Hex], respectively.

Simulation	**Systems**	**F-68**	**W**	[Ch]Cl	[Ch][Hex]
run5	F-68 + W	15	660000	–	–
run6	F-68 + [Ch]Cl + H_2O	15	660000	35412	–
run7	F-68 + [Ch][Hex] + H_2O	15	660000	–	15452
run8	L-35 + H_2O	15	173332	–	–
run9	L-35 + [Ch]Cl + H_2O	15	173332	3388	–
run10	L-35 + [Ch][Hex] + H_2O	15	173332	–	508

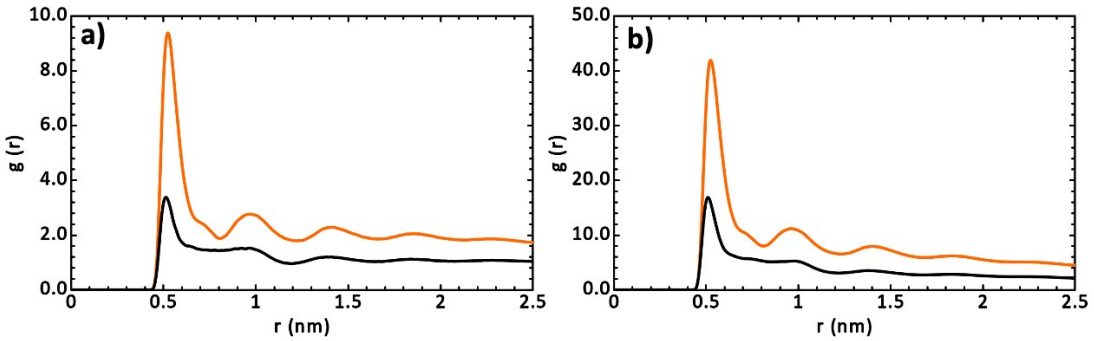

Figure S4. RDFs between the PEO-$[Ch]^+$ in orange and $[Hex]^-$-$[Ch]^+$ in black. a) F-68 and b) L-35 [Ch][Hex] ILs mixtures.

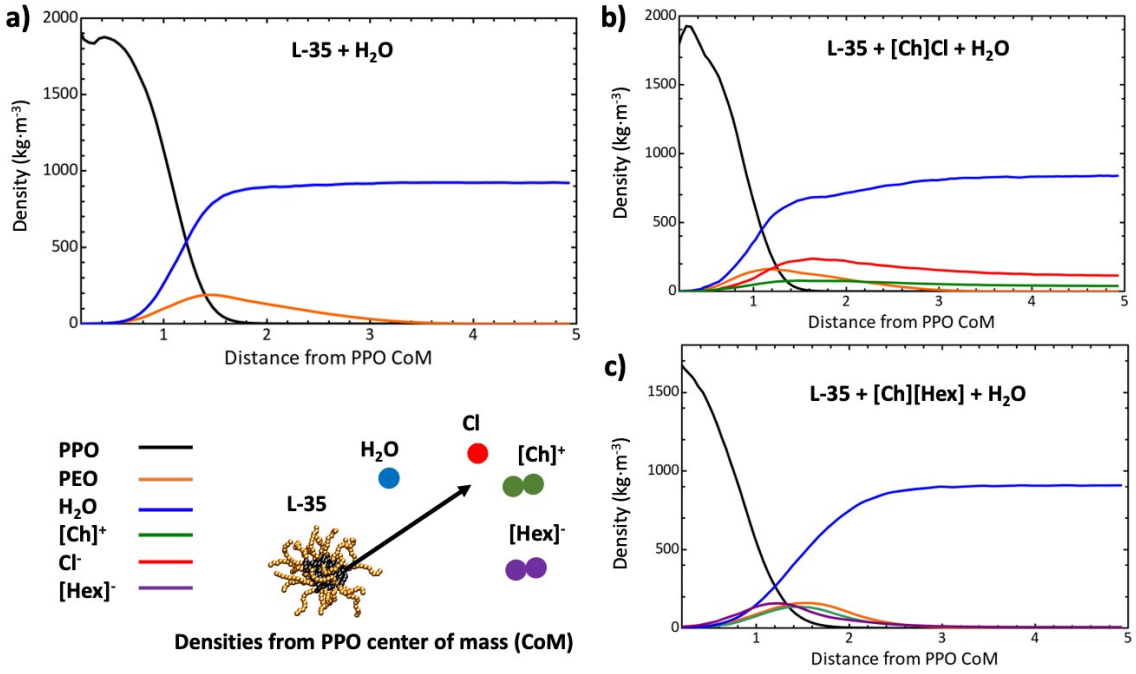

Figure S5. Density profiles for the L-35 aggregates taking the poly(propylene oxide) block (PPO) as the center of mass for the L-35 aqueous solution (run8) and their mixtures with [Ch]Cl (run9) and [Ch][Hex] (run10).

References:

1 S. J. Marrink, H. J. Risselada, S. Yefimov, D. P. Tieleman and A. H. de Vries, The MARTINI Force Field: Coarse Grained Model for Biomolecular Simulations, *J. Phys. Chem. B*, 2007, **111**, 7812–7824.

2 G. Pérez-Sánchez, J. R. B. Gomes and M. Jorge, Modeling Self-Assembly of Silica/Surfactant Mesostructures in the Templated Synthesis of Nanoporous Solids, *Langmuir*, 2013, **29**, 2387–2396.

3 G. Pérez-Sánchez, S.-C. Chien, J. R. B. Gomes, M. N. D. S. Cordeiro, S. M. Auerbach, P. A. Monson and M. Jorge, Multiscale Model for the Templated Synthesis of Mesoporous Silica: The Essential Role of Silica Oligomers, *Chem. Mater.*, 2016, **28**, 2715–2727.

4 S.-C. Chien, G. Pérez-Sánchez, J. R. B. Gomes, M. N. D. S. Cordeiro, M. Jorge, S. M. Auerbach and P. A. Monson, Molecular Simulations of the Synthesis of Periodic Mesoporous Silica Phases at High Surfactant Concentrations, *J. Phys. Chem. C*, 2017, **121**, 4564–4575.

5 S. Liu, D. Wu and X. Yang, Molecular Simulation Coarse-grained molecular simulation of self-assembly nanostructures of CTAB on nanoscale graphene Coarse-grained molecular simulation of self-assembly nanostructures of CTAB on nanoscale graphene, , DOI:10.1080/08927022.2015.1007053.

6 S. Illa-Tuset, D. C. Malaspina and J. Faraudo, Coarse-grained molecular dynamics simulation of the interface behaviour and self-assembly of CTAB cationic surfactants, *Phys. Chem. Chem. Phys.*, 2018, **20**, 26422–26430.

7 S. Soleimanzadegan, H. Farsi and F. Ebrahimi, Molecular dynamics simulation of some cyclic compounds solubilization into the nanometric core of Cetyltrimethylammonium Bromide micelle, *J. Mol. Struct.*, 2015, **1079**, 494–501.

8 T. I. Morrow and E. J. Maginn, Density, local composition and diffusivity of aqueous choline chloride solutions: a molecular dynamics study, *Fluid Phase Equilib.*, 2004, **217**, 97–104.

9 M. H. Ghatee, F. Ghanavati, M. Bahrami, A. R. Zolghadr, F. Borousan and Z. Fotouhabadi, Molecular Dynamics Simulation and Experimental Approach to the Temperature Dependent Surface and Bulk Properties of Hexanoic Acid, *Ind. Eng. Chem. Res.*, 2013, **52**, 3334–3341.